



Journal of Environmental Sciences

JOESE 5



Geotechnical studies using remote sensing and Cone penetration test at New Damietta: a case study

Ahmed El Shennawey ¹, Ahmed El Mahmoudi ¹ and Ayman Altahrany ²

¹Geology Department, Faculty of Science, Mansoura University

²Structural Department, Faculty of Engineering, Mansoura University

Reprint

Volume 49, Number 3: 64 - 71

(2020)

<http://Joese.mans.edu.eg>

P-ISSN 1110-192X

e-ISSN 2090-9233



Original Article

Geotechnical studies using remote sensing and Cone penetration test at New Damietta: a case study

Ahmed El Shennawy¹, Ahmed El Mahmoudi¹ and Ayman Altahrany²

¹Geology Department, Faculty of Science, Mansoura University

²Structural Department, Faculty of Engineering, Mansoura University

Article Info

Article history:

Received 24/ 5 /2020

Received in revised

form 29/7/2020

Accepted 30/8/2020

Keywords: *Land use land cover (LU-LC); Cone Penetration Test (CPTu); geotechnical parameters.*

Abstract

Egypt has recently witnessed a tremendous population increase, which has been accompanied by an expansion in the establishment of new cities along the coastal area and a rapid increase in urbanization such as New Mansoura, The new Administrative Capital, and New Damietta, which is the city of interest of this work. This city is suffering from saltwater intrusion and salinization problems. Some geotechnical problems appear because of the existence of certain phenomena which are not recognized by traditional geotechnical methods such as clay pockets. So, we introduce an integrative approach using remote sensing and Cone penetration test to evaluate the critical zone of problematic soil in the study area. Firstly, the land use land cover (LU-LC) is monitored from 1984 until now to understand the changes in sediment yield and land degradation over the analysis period. Thus, we could extract some features that disappear due to urban development, such as dunes and waterlogged areas. Then, we apply two Electric Cone Penetration Test (CPTu) with pore pressure measurements at two different major classes of LU-LC outputs. They provide us with a continuous and detailed stratigraphic profile. Furthermore, we can get initial estimates of geotechnical parameters that guide us in selective sampling for the critical zone. This gives us the chance to study seismic design, bearing capacity and settlement for shallow foundation design and other applications.

1. Introduction

In the last decade, Coastal cities are considered the most populated areas of the world, which host about a third of the world population (Cohen, Small, Mellinger, Gallup, & Sachs, 1997). This because the coastal zone contributes significantly to the national economy worldwide as a result of the abundance of existing natural resources (Turner, 2000). This led to an increase in urban extension and development through this region. On the other hand, there are coastal hazards that threaten urban growth in coastal areas such as regular flooding and other impacts of climate change (Nicholls, Hoozemans, & Marchand, 1999). Furthermore, all ecosystems are drastically affected by human activities that lead to extensive soil salinization and saltwater intrusion. So, the comprehensive understanding of subsurface soil properties is an essential goal for sustainable urbanism as intensive urban growth can magnify Geo-environmental hazards such as cracking, collapsing, and tilting in dramatic ways. Traditional geotechnical borings are expensive, time-consuming, and cannot get reliable soil parameters of the soil in its natural state. This because samples from the coastal area,

where the groundwater table located at shallow depths (60-90) cm, are extracted in a disturbed state. We applied our methodology at New Damietta as a case study located in the western part of the Damietta branch (Figure 1a). In the first stage, The land use-land cover (LU-LC) is introduced to get the changes in land degradation and sediment yield over the analysis period as the coastal area is characterized by the high rate of soil erosion and sediment deposition from day to day (Bagheri et al., 2019). Then, the Electric Cone Penetration Test (CPTu) was applied. The most significant advantage of this in situ test is that it allows the evaluation of the physical and mechanical characteristics of the soil in its natural state. It also has valuable benefits of overcoming disturbed samples to quantify soil properties, which cannot be determined from disturbed samples in traditional borings (Niazi & Mayne, 2016). It is also not dependent on the operator, unlike the standard penetration method (SPT) that is influenced by many human factors such as means of lifting and releasing the hammer and type of hammer used in the test (Eslami, Moshfeghi, MolaAbasi, & Eslami, 2019). Finally, It provides some empirical geotechnical

parameters such as relative density, Shear modulus and others which give us the chance to study seismic design and other applications.

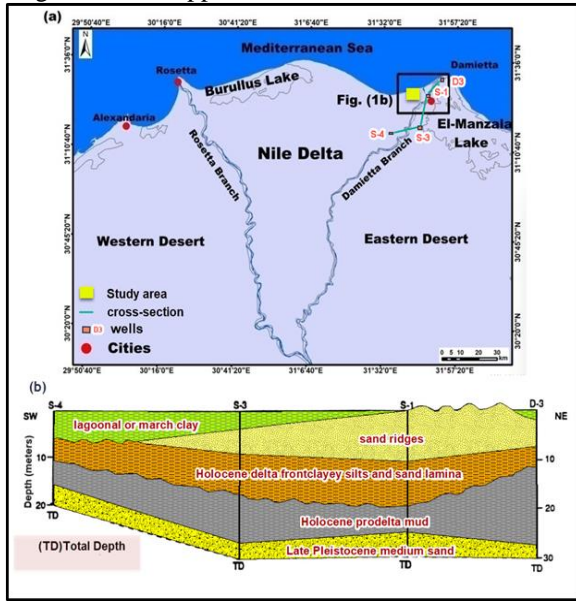


Figure 1: Location map of the study area showing (a) New Damietta City (Yellow box) along the Nile Delta, (b) Stratigraphic cross-section in the northeastern section of the Nile delta along the Damietta branch (SW-NE) modified after (Siegel, Gupta, Shergill, Stanley, & Gerber, 1995) and its location in (Figure 1a)

2. Local geology and soil

Since the study area is a part of the north region of the Nile delta, it shares most of its tectonic, geological, and hydrogeological setting. The geology of the delta is dominated by the Bilqas and the Mit Ghamr formations (Rizzini, Vezzani, Cococetta, & Milad, 1978). The Holocene subsurface stratigraphy was described as a progradation fluvio-marine sequence (Cutellier & Stanley, 1987; Stanley & Warne, 1993) and represented by Bilqas Formation. (Figure 1b) shows the Stratigraphic cross-section of the transect parallel to the studied area modified after (Siegel et al., 1995).

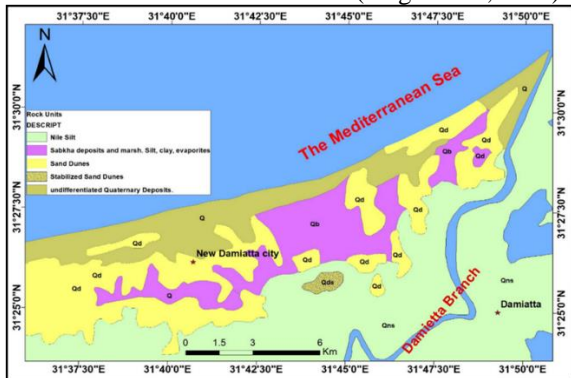


Figure 2: Surface geological map of the study area (CONOCO, 1987)

It consists of four wells (S-I, S-3, S-4, and D-3) and directed from land to sea (SW-NE). It shows the stratigraphic setting of the Holocene subsurface

stratigraphy contains the marine delta lobe facies and the deltaic Holocene facies. The marine delta lobe facies consist of the Pro delta and delta front mud and sand and reaches to a thickness of 20m. The deltaic Holocene sediments consist of coastal sand ridges, and the continental brackish mud of lagoons to marsh environment with thickness ranges from 1 to 18 m. Holocene sediments lie over late Pleistocene medium sand, which represented by Mit Ghamr formation. The study area is located in wadi plain sediments, where surface geology (Figure 2) is mainly composed of Quaternary sand dunes, sabkha deposits and clay (CONOCO, 1987).

**3. Data acquisition and processing
LU/LC analysis**

Satellite remote sensing images have been used successfully to detect physiographic changes in the coastal zone, including land use/land cover (LU/LC) changes (Taha & El-Asmar, 2019). Digital change detection is a method of defining changes in land-cover and land-use properties based on multi-temporal remote sensing data. In the present research, two different types of Landsat images were collected from the website of the United States Geological Survey (USGS, 2019): one from the Landsat 5, the thematic mapper (TM), acquired in 1984 and one from Landsat 8, the operational land imager (OLI), acquired in 2019.

They were used to classify the land cover in the study area, over 35 years. All image scenes were subjected to image processing using ERDAS Imagine software version 6.1. Supervised classification was applied for two images (1984 and 2019) through ERDAS Imagine by maximum likelihood classifier by support vector machine algorithm was made for the classification to categorize the existing classes based on their spectral properties. Then, changes in geomorphic units were detected in the study area due to human and natural activities with the change detection tool.

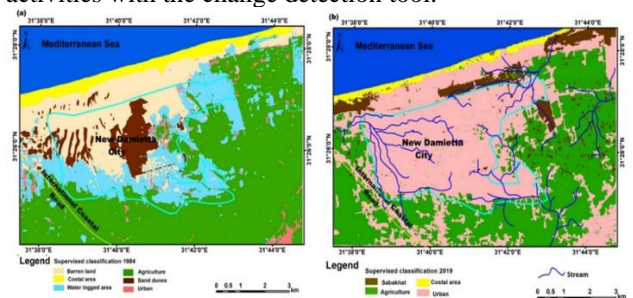


Figure 3. (a) Supervised classification for Landsat image 1984 shows the Geomorphological unit of the new Damietta city and surrounding areas. (b) Supervised classification for Landsat image 2019

Accordingly, six land cover classes for the image of 1984 were identified, as shown in (Figure 3a): Waterlogged area, agriculture, urban, coastal area, barren land, and dunes Whereas, the outcome classification of 2019 image in (Figure 3b). It is attributed to four land-cover classes, including

sabkha (salt-flat), urban, agriculture, and coastal area. The increase in land reclamation and urbanization with time reduce the areas of most geomorphologic units such as sand dunes, wetland, and sabkhas.

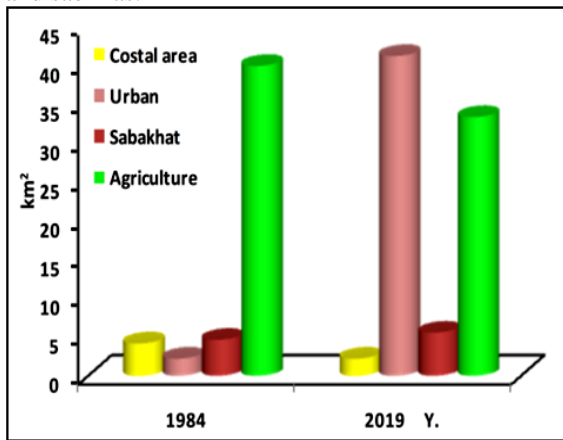


Figure 4. Change detection histogram in the study area.

Overall, through 35 years from 1984 to 2019, the urban area experience wide distribution over the study area at the expense of some landforms, which reduced significantly, especially sand dunes. The resulted histogram from change detection analysis (Figure 4) showed that Urban land and sabkha increased from less than 5 km² for both in 1984 to 45 km² and 7 km² in 2019, respectively. Agriculture land and coastal land decreased during this period from 45 km² and 5 km² in 1984 to 35 km² and 2 km² in 2019, respectively (Figure 4). Recently, as seen in the 2019 Landsat image, most of the quaternary sand dunes have dwindled with a rapid rate of new-urban areas development induced by human activities and includes land reclamation, urbanization, and road construction. They cover 1.1 to 1.4 km in length, with their long extension parallel to the dominant wind in N and NW directions. The waterlogged area is observed on a large scale through the studied area. The area of this landform diminishes intensely due to urban expansion and cultivated land. Sabkhas are very limited and cover about 5 km² close to the coast in the northeastern part of the studied area (Figure 3b).

Geotechnical measurements

During Feb. 2020, Two cone penetration tests (CPT) were performed with pore pressure measurement (CPTu) following the Active Standard Test Method (ASTM D 5778, 2012) at different locations, as shown in Figure 5b. The first one was performed in the northern part at sand dune location until 38 m depth. The other was applied in the southern part on the waterlogged area and was continued to 33 m depth.

The used rig (TG 73-200 KN) works with a four-cylinder diesel engine which provides 36 HP of power. The rig is running on wheels and tracks to set up at the required position with a velocity of 2 Km/hour. The hydraulic jack will be applying for

self-levelling the rig, and the auger will be used with a maximum torque of 500 kg m to achieve the fixation on the surface of the ground and to produce the reaction load needed. The rig capacity is 20 tons with 20 mm / sec of cone penetration rate. The used cone has an apex angle of 60 degrees. The projected base area of the cone is 10 cm².

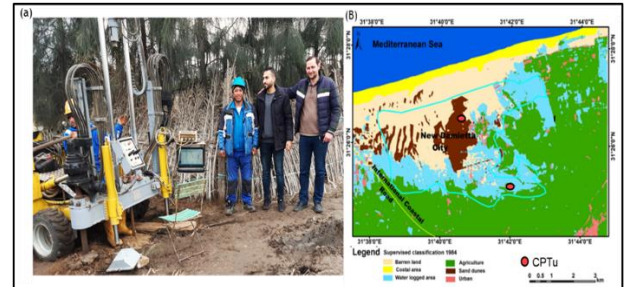


Figure 5: (a) shows one of the field photos for applying CPTu sounding with our teamwork. (b) The location map of two CPTu soundings with LU-LC outputs.

The base of the cone has an equal outside diameter of the shaft section with a sleeve surface area of 150 cm². The thrust system should be set up to get a direction of thrust as close to vertical as possible. The initial thrust path deviation from vertical should not exceed 2 degrees, and the pushrods should be tested. The cone will be advanced with a constant rate of two centimeters per second while recording cone resistance (q_c), sleeve resistance (f_s) and pore water pressure (u₂) data every 2 cm using electrical data acquisition equipment and a portable computer. The test was continued to the required depth or refusal. Figure 5a shows one of the field photos for proceeding CPTu sounding. These measured parameters are presented graphically (Figure 6), including q_c, f_s, and u₂ versus depth using CPET-IT v.1.7.6.3 software, which also used for data processing and interpretation.

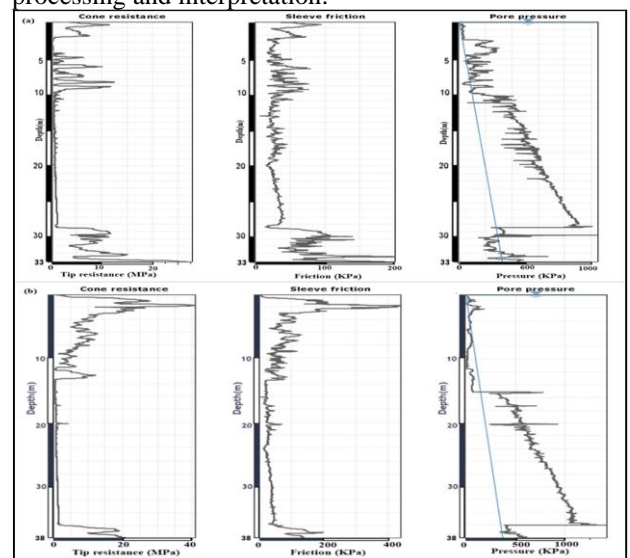


Figure 6 shows a graphical representation of measured parameters from CPTu soundings (a) CPTu is located at the south with 33m depth (b) second CPTu sounding at the north with 38m depth.

Firstly, the measured cone resistance is corrected for water pressure effect due to the unequal end area effect of the exposed surface behind the cone (Campanella et al., 1982) particularly for both soft clay and silt but in sandy soil $q_c = q_t$. We apply this relation;

$$q_t = q_c + u_2 (1 - a).$$

Where (q_t) = corrected total cone tip resistance, (q_c) = measured cone resistance, u_2 = measured water pressure at the base of sleeve & 'a' is the net area ratio (AN/AT) determined from laboratory calibration, which equal [load transfer area behind the cone tip (AN)/ cross-sectional area at the base of cone tip (AT)], with a typical value between 0.70 and 0.85.

since these measured cone parameters increased with depth because of the rise in effective overburden stress, normalized (dimensionless) CPT data includes [Q_{tn} (normalized cone penetration resistance), F_r (normalized friction ratio, in %), B_q (normalized pore pressure)] for overburden stress is required to estimate soil behaviour type (SBT) and other empirical geotechnical parameters, where;

$$Q_{tn} = [(q_t - \sigma_{vo}) / P_a] / (P_a / \sigma'_{vo})^n$$

$$F_r = (f_s / (q_t - \sigma_{vo})) \times 100\%$$

$$B_q = \Delta u / (q_t - \sigma_{vo})$$

Where Δu is excess penetration pore pressure; (σ_{vo}) in-situ total vertical stress; and (σ'_{vo}) in-situ effective vertical stress. $(q_t - \sigma_{vo}) / P_a$ is the dimensionless net cone resistance; $(P_a / \sigma'_{vo})^n$ is the stress normalization factor; P_a is the atmospheric pressure in the same units as q_t and σ_{vo} , and n is the stress exponent that varies with SBTn

4. Results and discussion

Soil behaviour classification (SBC) Using CPTu sounding

The normalized cone parameters can be combined into one soil behaviour Type index, I_c , to estimate soil behaviour type (Figure 7&8) providing us with continuous stratigraphy profile using normalized SBTn charts based on either $Q_t - F_r$ and $Q_t - B_q$ (Robertson, Woeller, & Finn, 1992, updated by Robertson, 2010). I_c represents the radius of the substantially concentric circles that represent the boundaries between SBTn zones. I_c can be defined as follows;

$$I_c = ((3.47 - \log Q_m)^2 + (\log F_r + 1.22)^2)^{0.5}$$

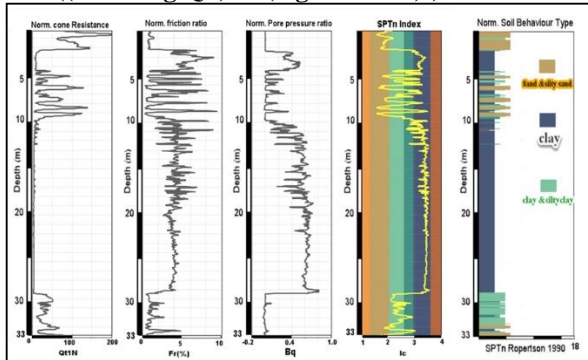


Figure 7 shows the results of Soil behaviour classification (SBC) Using CPTu sounding in the

southern part of the study site at the waterlogged area.

Regarding the second CPTu that located in the north, Figure 8 represents the soil behaviour type of 38m depth profile. It also shows the same characteristic of the clay layer of the first profile with the same value of excess pore pressure and cone and sleeve resistance, which indicate the same fluvial marine environment of deltic deposits. The clay layer is overlain by a thick sand layer that attributed to sand ridge deposits. This sandy layer is relatively similar to the first layer in the south profile, but have higher cone resistance.

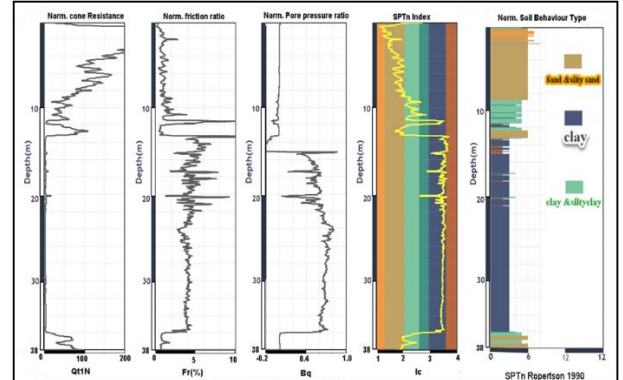


Figure 8 shows the results of Soil behaviour classification (SBC) Using CPTu sounding in the northern part of the study site at sand dune area

Estimate soil parameters

We established numerous semi-empirical correlations to estimate CPT geotechnical properties for different types of soils.

Cone penetration is typically undrained in fine-grained soils, such as clays and silts. This applies only to 1,2,3,4 and 9 of SBTn zones. When cone penetration tests are carried out under undrained conditions, pore pressure is generated, which affects the measurement of both cone resistance and sleeve friction. The measurement of pore pressure is hugely beneficial as it used for the interpretation of soil parameter analysis. Furthermore, Cone resistance and sleeve friction must be corrected using the measured pore pressures (Abu-Farsakh et al., 2003). On the other hand, Cone penetration testing is generally drained in coarse-grained soils, such as sandy soils. This applies only to 5,6,7 and 8 of SBTn zones. No excess pore pressures should be generated under drained conditions, and the in situ static pore pressure is only measured. When Fully drained cone penetration is considered, the only measured cone resistance and sleeve friction are included in the interpretation in terms of soil parameters. However, It is essential to review the recorded pore pressures to check whether the assumption of fully drained conditions is valid (Lunne et al., 2002).

1. In- situ state characteristics:

In Fine-grained soil:

- Overconsolidation Ratio (OCR) – Stress history

In geotechnical practice, OCR is defined as the ratio of the maximum past effective consolidation stress (σ'_p) and the current effective overburden (vertical) stress (σ'_{vo}). The most simplified theory to determine OCR based on hybrid theoretical methods by (Kulhawy & Mayne, 1990) as follows:

$$OCR = K \left(\frac{q_t - \sigma'_{vo}}{\sigma'_{vo}} \right) = K Q_t$$

Where (Q_t) is normalized cone resistance, and K is a constant defined by the user. We apply the average value of $k = 0.33$ for this study. Figure 9 shows the OCR results of two CPTu soundings. Most of the clay interpreted as normally consolidated clay, where the values less than two. Small beds behave as overconsolidated clay where the value larger than 5, which mainly appears in southern CPTu sounding (Figure 9b).

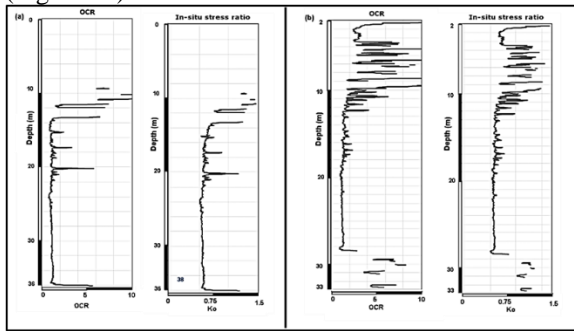


Figure 9 shows the profile of the Overconsolidation Ratio (OCR) and in-situ stress ratio for both CPTu soundings (a) CPTu in the northern part (b) CPTu in the southern part.

➤ **In-Situ Stress Ratio (K_o)**

(Kulhawy & Mayne, 1990) introduced a more straightforward approach to estimate K_o from CPT which is

$$K_o = 0.1 \left(\frac{q_t - \sigma'_v}{\sigma'_{vo}} \right)$$

Figure 9 shows the In-Situ Stress Ratio profile for both soundings. It is about 0.5, which indicate the dominance of soft clay. There are little parts in the southern profile that reaches to 1.5, which indicate the lightly stiff clay.

In coarse-grained soil :

➤ **Relative Density (Dr)**

Because of the limitations of use in the in situ state of density tests that can only be applied at shallow depth, the use of CPT records to assess Dr based on large calibration chamber (cc) testing. (Kulhawy & Mayne, 1990) suggested a more straightforward relationship for estimating relative density for most young, uncemented silica-based sands to:

$$Dr(\%) = 100 \sqrt{\frac{Q_{tn}}{K_{DR}}}$$

Where relative density constant, $K_{Dr} = 350.0$. This relationship was applied to our CPTu records, and the resulted profiles appear in Figure 10. They indicate medium to loose sand in the study area.

When the value higher than 50, it pretty dense in small parts of the profile.

➤ **State Parameter (ψ)**

The state parameter (ψ) is defined as the difference between the current void ratio, e , and the void ratio at critical state e_{cs} , at the same mean effective stress for sandy soils (Robertson, 2010). (Robertson & Cabal, 2010) suggested a simplified and approximate relationship between ψ and the clean sand equivalent normalized cone resistance, $Q_{m,cs}$, as follows:

$$\psi = 0.56 - 0.33 * \log(Q_{tn,cs})$$

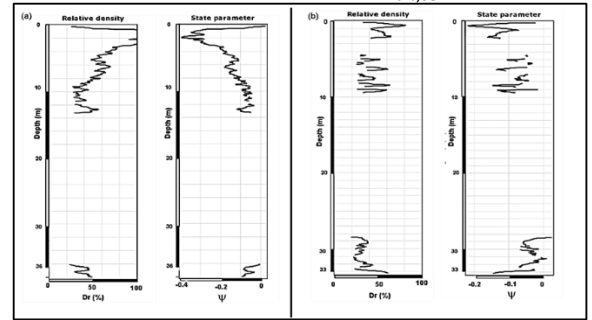


Figure 10 shows the profile of Relative Density (Dr) and state parameter (ψ) for both CPTu soundings (a) CPTu in the northern part (b) CPTu in the southern part.

Figure 10 shows the resulted profile of the state parameter for both soundings. It is showing the negative values of the state parameter with average equals to -0.2. This indicates a dilative state of medium sand at low confining pressure, and the void ratio is less than the void ratio of critical state at the same confining pressure. In the northern profile, it reaches in small part at -0.4 which indicates dense sand. In the southern profile, it reaches to zero in some location, which indicates the sand become loose.

2. Strength characteristics:

In Fine-grained soil:

➤ **Undrained Shear Strength (s_u)**

It is formally called cohesion (c) and examined for stability and bearing capacity assessment (Eslami et al., 2020).

Several theoretical solutions have been developed by the aid of empirical correlations in the form of a simple relationship of net cone resistance divided by an undrained shear strength cone factor for clay (N_{kt}). Typically, this constant factor ranges from 10 to 18, with 14 as an average for $S_{u(ave)}$. In this study, $S_{u(ave)}$ is applied as a bearing factor (N_{KT}). So, the evaluation of (s_u) from CPT soundings is applied using the following relation;

$$s_u = \frac{(q_t - \sigma'_v)}{N_{KT}}$$

Figure 11 shows the resulted profile of undrained shear strength which represented by the black line. It is also called peak undrained shear strength. On the other hand, the red line represents the remoulded shear strength $S_{u(rem)}$, which is defined as the magnitude of the shear stress that a disturbed soil can

bear in an undrained condition. $S_{u(rem)}$ essentially equals to sleeve friction (f_s) (Lunne, Robertson, & Powell, 1997) as shown in the following equation;

$$S_{u(rem)} = f_s$$

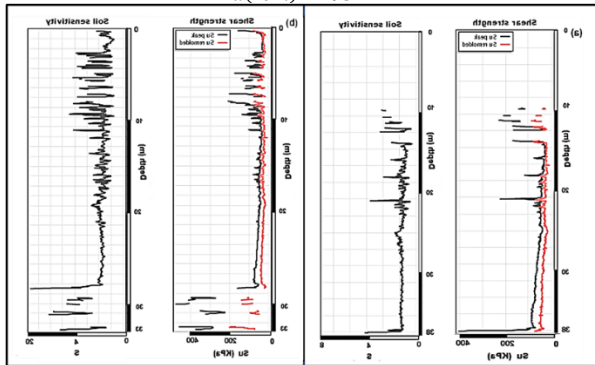


Figure 11 shows the profile of undrained shear strength (S_u) and Soil Sensitivity (S_t) for both CPTu soundings (a) CPTu in the northern part (b) CPTu in the southern part.

The resulted profile of shear strength shows remoulded undrained shear strength $S_{u(rem)}$ values is less than 50 KPa in most of the profiles and higher than 50 in small locations for both CPTu soundings (Figure 11). This usually indicates Normally consolidated (NC) clay to lightly overconsolidated clay (LOC) that dominates in both of two profiles, but the sensitivity gets higher when $S_{u(rem)}$ becomes smaller. There are quite variable between in stiff and soft clay in small locations.

➤ **Soil Sensitivity (S_t)**

The sensitivity (S_t) can be defined as the ratio of undisturbed peak undrained shear strength(S_u) to remoulded undrained shear strength $S_{u(rem)}$ (Mayne, 2014). the sensitivity of fine-grained soil can be estimated using the following relation;

$$S_t = \frac{N_s}{F_r}$$

Where N_s is a constant, and F_r is the friction ratio. We define constant =7 based on $N_{KT} = 14$. Figure 11 shows the sensitivity of the two profiles. The average values for both profiles lie between 2 and 1, which indicate the slightly sensitive clay as the one indicates insensitive clay.

3. Deformation characteristics

➤ **small strain shear modulus(G_0) and Estimating Shear Wave Velocity(V_s)**

Shear wave velocity (V_s) induced shear modulus (G_0), known as a critical geotechnical parameter, corresponded to a small strain that is important for earthquake studies (Eslami et al., 2020). Hence, G_0 for young, uncemented soils can be estimated using:

$G_0 = 0.0188 [10^{(0.55I_c + 1.68)}] (q_t - \sigma_{vo})$
 At low shear strain levels (less than about 10-4%), the shear modulus in soils is constant and has a maximum value, G_0 . The shear wave velocity is determined from small strain shear modulus using the equation:

$$G_0 = \rho(V_s)^2$$

Where ρ is the mass density. Figure 12 shows that shear wave velocity is less than 250 m/s that indicates most Holocene age deposits. When V_s increases in small parts of the profile, it indicates the resistance of loading goes up and small strain behaviour.

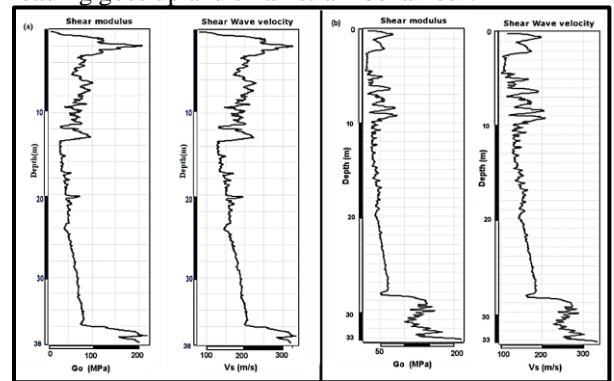


Figure 12 shows the profile of small strain shear modulus and Estimating Shear Wave Velocity for both CPTu soundings (a) CPTu in the northern part (b) CPTu in the southern part.

Conclusion

The LU-LC analysis provides us with the image of the paleoenvironment, which is significant to understand the environmental conditions and its implication on the geotechnical setting. CPTu enables us to estimate some empirical geotechnical parameters that have repeatability and reliability than other traditional geotechnical techniques. This gives us the chance to detect the critical zone for focused study and selective sampling. The representation of soil parameters as profiles enables us to feel variability relative to the stratigraphic profile and understand the situation much better than traditional methods. These parameters enable us to study settlement, liquefaction and seismic design for shallow and deep foundations. This will act as a helpful guide for the engineers and decision-makers in the planning and constructions processes, which lead to sustainable urbanism.

5. References:

Abu-Farsakh, M., Tumay, M., & Voyiadjis, G. (2003). Numerical parametric study of piezocone penetration test in clays. International Journal of Geomechanics, 3(2), 170-181.

American Society for Testing and Materials. (2012). Standard test method for electronic friction cone and piezocone penetration testing of soils. ASTM International.

Bagheri, M., Ibrahim, Z. Z., Mansor, S. B., Abd Manaf, L., Badarulzaman, N., & Vaghefi, N. (2019). Shoreline change analysis and erosion prediction using historical data of Kuala Terengganu, Malaysia. Environmental Earth Sciences, 78(15), 477.

Cohen, J. E., Small, C., Mellinger, A., Gallup, J., & Sachs, J. (1997). Estimates of coastal populations. Science, 278(5341), 1209-1213.

CONOCO, E. C. (1987). Geological map of Egypt (Cairo sheet). Scale 1:500,000.

Coutellier, V., & Stanley, D. J. (1987). Late Quaternary stratigraphy and paleogeography of the eastern Nile Delta, Egypt. *Marine geology*, 77(3-4), 257-275.

Campanella, R. G., Gillespie, D., & Robertson, P. (1982). Pore pressures during cone penetration testing. [No source information available].

Eslami, A., Moshfeghi, S., MolaAbasi, H., & Eslami, M. M. (2019). Piezocone and Cone Penetration Test (CPTu and CPT) Applications in Foundation Engineering. Butterworth-Heinemann.

Eslami, A., Moshfeghi, S., MolaAbasi, H., & Eslami, M. M. (2020). 4 - Geotechnical parameters from CPT records. In A. Eslami, S. Moshfeghi, H. MolaAbasi, & M. M. Eslami (Eds.), *Piezocone and Cone Penetration Test (CPTu and CPT) Applications in Foundation Engineering* (pp. 81-110): Butterworth-Heinemann.

Kulhawy, F. H., & Mayne, P. W. (1990). Manual on estimating soil properties for foundation design (No. EPRI-EL-6800). Electric Power Research Inst., Palo Alto, CA (USA); Cornell Univ., Ithaca, NY (USA). Geotechnical Engineering Group.

Niazi, F., & Mayne, P. (2016). CPTu-based enhanced UniCone method for pile capacity. *Engineering Geology*, 212. doi: 10.1016/j.enggeo.2016.07.010

USGS. (2019). EarthExplorer website for downloading satellite remote sensing data. Retrieved from <https://earthexplorer.usgs.gov/> (Last access 9th January 2019)

Lunne, T., Powell, J. J., & Robertson, P. K. (2002). Cone penetration testing in geotechnical practice. CRC Press. Massarsch, K. R. (2014). 2014 Cone penetration testing.

Lunne, T., Robertson, P. K., & Powell, J. J. M. (1997). Cone penetration testing in geotechnical practice. Blackie Academic. Chapman.

Mayne, P. W. (2014). Generalized CPT method for evaluating yield stress in soils. In *Geo-Congress 2014: Geo-Characterization and Modeling for Sustainability* (pp. 1336-1346).

Nicholls, R. J., Hoozemans, F. M., & Marchand, M. (1999). Increasing flood risk and wetland losses due to global sea-level rise: regional and global analyses. *Global Environmental Change*, 9, S69-S87.

Niazi, F., & Mayne, P. (2016). CPTu-based enhanced UniCone method for pile capacity. *Engineering Geology*, 212. doi: 10.1016/j.enggeo.2016.07.010

Robertson, P., Woeller, D., & Finn, W. J. C. G. J. (1992). Seismic cone penetration test for evaluating liquefaction potential under cyclic loading. 29(4), 686-695.

Robertson, P. K., & Cabal, K. L. (2010). Guide to cone penetration testing for geotechnical engineering. Gregg Drilling & Testing.

Robertson, P. K. (2010, May). Estimating in-situ state parameter and friction angle in sandy soils from CPT. In 2nd International Symposium on Cone Penetration Testing (pp. 2-43).

Rizzini, A., Vezzani, F., Cococetta, V., & Milad, G. (1978). Stratigraphy and sedimentation of a Neogene—Quaternary section in the Nile Delta area (ARE). *Marine Geology*, 27(3-4), 327-348.

Siegel, F. R., Gupta, N., Shergill, B., Stanley, D. J., & Gerber, C. (1995). Geochemistry of Holocene sediments from the Nile Delta. *Journal of coastal research*, 415-431.

Stanley, D. J., & Warne, A. G. (1993). Nile Delta: recent geological evolution and human impact. *Science*, 260(5108), 628-634.

Taha, M. M., & El-Asmar, H. M. (2019). Geo-Archeoheritage Sites Are at Risk, the Manzala Lagoon, NE Nile Delta Coast, Egypt. *Geoheritage*, 11(2), 441-457.

Turner, R. K. (2000). Integrating natural and socio-economic science in coastal management. *Journal of marine systems*, 25(3-4), 447-460.